engineering proceedings

MDPI

Proceeding Paper

Automated Control of Dynamic Loads in Drive Systems †

Alina Fazylova [1,*], Kuanysh Alipbayev [1], Teodor Iliev [2] and Alisher Aden [1]

[1] Department of Electronic Engineering, Almaty University of Power Engineering and Telecommunications Named After G. Daukeev, Almaty 05000, Kazakhstan; k.alipbayev@aues.kz (K.A.); a.aden@aues.kz (A.A.)
[2] Department of Telecommunications, University of Ruse, 7004 Ruse, Bulgaria; tiliev@uni-ruse.bg
* Correspondence: a.fazylova@aues.kz; Tel.: +7-7058079062
† Presented at the International Conference on Electronics, Engineering Physics and Earth Science (EEPES 2025), Alexandroupolis, Greece, 18–20 June 2025.

Abstract

This article discusses the automated control of dynamic loads in drive systems using the example of a wind turbine screw drive. A mathematical model was developed, including differential equations of system motion, the voltage balance of the electric motor, and transfer functions of the control system. The Laplace transform was applied to obtain the system's frequency and time characteristics. Numerical calculations and simulation results are presented, demonstrating the system's stability and the effectiveness of the proposed control method. The generated amplitude–frequency and transient response graphs confirm the system's operability. The proposed approach enhances the reliability of the screw drive, reduces mechanical loads, and extends the equipment's service life.

Keywords: control scheme; feedback; automatic regulation; vertical-axis wind turbine; transfer function

1. Introduction

Wind energy is one of the most promising areas in the field of renewable energy, offering an environmentally friendly and sustainable way of generating electricity. The efficiency and reliability of wind turbines largely depend on their ability to adapt to dynamic environmental conditions, including changes in wind speed and direction. In this context, the development and implementation of adaptive control systems are key to optimizing the performance and extending the service life of wind turbines. Among modern approaches to adaptive wind turbine control, several key directions can be distinguished: pitch control [1], which increases energy conversion efficiency but requires complex mechanisms and regular maintenance; variable speed control [2], which maintains an optimal power coefficient and reduces dynamic loads, though it complicates control systems and increases demands on drive components; and the use of intelligent control systems, such as neural networks and adaptive fuzzy controllers [3], which provide high adaptability but require significant computational resources and complex configuration. A promising direction is automatic rotor height regulation [4], which involves adjusting the rotor height of the wind turbine based on wind parameters. This allows for energy capture optimization and reduced turbulence effects. Advantages include the ability to operate across a broader range of wind conditions and reduced mechanical stress on the structure. However, implementing such systems requires complex mechanical solutions and may increase the mass and cost of the installation. Each of these methods has its own advantages and limitations. Pitch and variable speed control allow effective

check for updates

Academic Editor: Grigor Mihaylov

Published: 4 September 2025

Citation: Fazylova, A.; Alipbayev, K.; Iliev, T.; Aden, A. Automated Control of Dynamic Loads in Drive Systems. *Eng. Proc.* **2025**, *104*, 76. https://doi.org/10.3390/engproc2025104076

Copyright: © 2025 by the authors. Licensee MDPI, Basel, Switzerland. This article is an open access article distributed under the terms and conditions of the Creative Commons Attribution (CC BY) license (https://creativecommons.org/licenses/by/4.0/).

adaptation to changing wind conditions but require complex and costly control systems and mechanical components [1]. Intelligent control systems offer a high level of adaptability, but their implementation is associated with additional costs for computational resources and tuning [5]. Automatic rotor height regulation represents a promising approach for optimal rotor positioning under various conditions, but further research is required to overcome technical and economic challenges [6].

The aim of this study is to develop an automatic rotor height regulation system for a Vertical-Axis Wind Turbine (VAWT) using a screw drive, based on the principles of adaptive control. The work will include an analysis of existing technologies, the development of a mathematical model of the system, and an assessment of its performance under various operating conditions. The proposed approach is expected to improve energy conversion efficiency and reduce dynamic loads on the structure, thereby increasing the reliability and longevity of wind turbines. In this project, the rotor height adjustment mechanism is implemented through a ball screw drive model HIWIN R32-10A, chosen for its high load capacity, precision, and efficiency in vertical positioning systems, which ensures stable operation under varying aerodynamic loads. The control system is built on a microcontroller ARM Cortex-M0+ (RP2040) from the Raspberry Pi Foundation, programmed using C/C++ SDK or MicroPython (via Thonny IDE or Visual Studio Code), providing sufficient computational resources for adaptive algorithms while maintaining energy efficiency.

2. Materials and Methods

Figure 1 shows the automatic rotor height regulation system of an off-grid wind turbine 600 W with Darrieus & Savonius, manufactured by TYPMAR, Shenzhen, China model CXF-600W using a ball screw drive produced by HIWIN in Offenburg, Germany, model R32-10A. The operating principle is based on adaptive height control depending on wind speed. The airflow (1) impacts the anemometer (2), which measures wind speed and direction and transmits the data to the microcontroller ARM Cortex-M0+ (RP2040) from the Raspberry Pi Foundation (3) [7]. The embedded software programmed Python 3.11 analyzes the received data and makes decisions regarding rotor height adjustment. A frequency converter (4) is used to control the height by regulating the voltage supplied to the screw drive electric motor (5). The electric motor activates the screw mechanism, smoothly changing the position of the rotor (6) to enhance operational efficiency or provide overload protection.

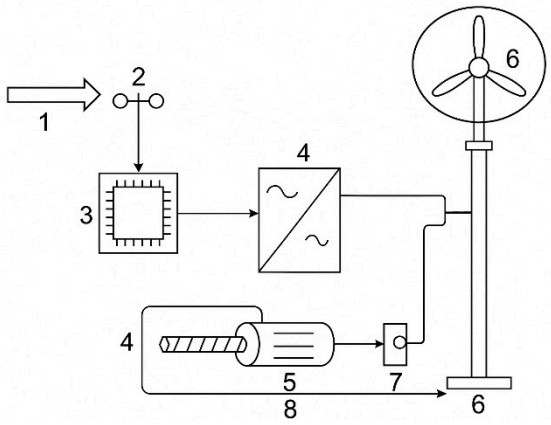


Figure 1. General control system diagram.

The system is equipped with a feedback mechanism that includes a position potentiometer (7), which records the current rotor position and sends a signal through the feedback loop (8) to the microcontroller (3). This enables precise movement control and

minimizes excessive adjustments. The automation of the height control process reduces the need for manual intervention, extends equipment service life, and enhances the reliability of wind turbine operation under changing weather conditions.

During the operation of a wind turbine, its rotor is subjected to various external loads, including aerodynamic forces from the wind flow, gravitational forces, and forces arising within the drive mechanism. Optimizing the system's performance requires an accurate mathematical description of the rotor's motion, which enables the prediction of its behavior under different operating conditions and the development of effective control algorithms [8].

One of the key equations describing the rotor's vertical motion is a differential equation based on Newton's second law. This law states that the net force acting on an object is equal to the product of its mass and acceleration [9]:

$$m\frac{d^2x}{dt^2} = F_{np} - F_{T_P} - mg, \tag{1}$$

where $x(t)$—vertical position of the rotor; m—mass of the rotor (20 kg); g—acceleration due to gravity (9.81 m/s^2); $F_{applied}$—force generated by the screw drive; $F_{friction}$—friction force.

The force $F_{applied}$ can be expressed through the motor torque. Based on the condition of motion transmission through the screw drive [10]:

$$F_{applied} = \frac{2M}{d_2} \cdot \eta_{screw}, \tag{2}$$

where M—motor torque; d_2—mean diameter of the screw; η_{screw}—efficiency of the screw drive.

Substituting this into the equation of motion gives the following [8]:

$$m\frac{d^2x}{dt^2} = \frac{2M}{d_2} \cdot \eta_{screw} - F_{friction} - mg, \tag{3}$$

Next, the friction force in the thread was expressed, which includes two components: dry friction, dependent on the normal force N, and viscous friction, proportional to velocity. The normal force is determined through the load force, allowing both types of resistance to be comprehensively accounted for in the mechanical model:

$$N = \frac{mg}{cos\alpha} \tag{4}$$

Thread friction is calculated using the formula [11]

$$F_{friction} = fN + b\frac{dx}{dt} \tag{5}$$

where f—coefficient of dry friction; N—normal force; b—coefficient of viscous friction, dx/dt—velocity of the rotor.

By substituting into the main equation of motion, the following was obtained:

$$m\frac{d^2x}{dt^2} = \frac{2M}{d_2} \cdot \eta_{screw} - f\frac{mg}{cos\alpha} - b\frac{dx}{dt} - mg \tag{6}$$

The second-order differential equation given by Formula (6) describes the rotor's motion. Since the movement is defined by the motor's rotation angle $\theta(t)$, it is possible

to proceed with calculations using angular variables. The relationship between linear displacement and angular rotation is given as follows [12]:

$$x = P\theta \tag{7}$$

Next, differentiation was performed twice:

$$\frac{dx}{dt} = p\frac{d\theta}{dt};\ \frac{d^2x}{dt^2} = p\frac{d^2\theta}{dt^2} \tag{8}$$

The obtained values were then substituted into Equation (6):

$$m\frac{d^2\theta}{dt^2} = \frac{2M}{d_2}\cdot\eta_{screw} - f\frac{mg}{cos\alpha} - bp\frac{d^2\theta}{dt^2} - mg \tag{9}$$

For the effective control of the wind turbine's screw drive, it is essential to consider the dynamics of the electric motor, which serves as the primary component for converting electrical energy into mechanical motion. The electric motor controls the screw drive by adjusting its speed and generating the torque required to raise or lower the rotor. To accurately describe the processes occurring within the motor, a mathematical equation based on electrical circuit laws is used. When the motor is powered by direct or alternating current, its winding follows the fundamental voltage balance equation, which accounts for the winding resistance, inductance, and back electromotive force (EMF). This equation determines the relationship between the current in the winding, the applied voltage, and the rotor's rotational speed. The fundamental equation of the motor armature electrical circuit is given by [11]

$$U = R_i + L\frac{d_i}{dt} + k_e\omega \tag{10}$$

The electric motor is the key component in controlling the screw drive, converting electrical energy into mechanical work. It is important to consider its characteristics to determine how changes in input parameters (voltage, current) affect the generated torque, angular velocity, and, consequently, the overall movement of the system. The screw drive controls the displacement of the wind turbine rotor, and its behavior is governed by several interrelated equations: the torque equation, the angular velocity equation, and the voltage balance equation in the motor circuit. Incorporating these equations into the dynamic model of the system allows for the analysis of the mechanism's operation and the development of effective control algorithms. The torque generated by the motor is defined by the following relationship [12]:

$$M = k_m i \tag{11}$$

This equation shows that the torque is linearly dependent on the current flowing through the motor winding. By controlling the current, it is possible to regulate the rotational dynamics of the motor. The relationship for angular velocity is given by [13]

$$\omega = \frac{d\theta}{dt} \tag{12}$$

This is a fundamental relationship that links the rotational speed to the shaft's angle of rotation. Using this expression allows for consideration of the system's kinematic characteristics. By applying Kirchhoff's law to the motor winding's electrical circuit, the following can be written [14]:

$$U = R\frac{M}{k_m} + L\frac{d}{dt}\left(\frac{M}{k_m}\right) + k_e\frac{d\theta}{dt} \tag{13}$$

This equation shows how the voltage across the motor winding varies depending on resistance, inductance, and back EMF. It allows for accounting for the influence of all electrical parameters on the motor's operation. After transforming Equation (12), the motor equation was obtained:

$$L\frac{d}{dt} + RM + k_e k_m \frac{d\theta}{dt} = k_m U \tag{14}$$

This differential equation describes the dynamic behavior of the motor under varying input voltage. In accordance with Equation (8), the screw drive motion equation takes the following form:

$$mp + bp\frac{d\theta}{dt} + mg = \frac{2M}{d_2} \cdot \eta_{screw} - f\frac{mg}{cos\alpha} \tag{15}$$

The presented equations form the foundation for analyzing the electromechanical system of the screw drive. They illustrate how voltage, current, torque, and angular velocity interact within the system, influencing the rotor's displacement. Further analysis and modeling of these equations enable the optimization of system control, ensuring the precise and efficient regulation of the wind turbine rotor's height.

3. Results and Discussion

To analyze the dynamic characteristics of the screw drive and the rotor height control system of the wind turbine, it is convenient to transform the differential equations into the operational form using the Laplace transform. This approach allows the system to be represented by transfer functions, which significantly simplifies the analysis of its behavior in the frequency domain and facilitates the development of control algorithms and the assessment of system stability. The Laplace transform is applied to the rotor motion and electric motor equations, resulting in a system of algebraic equations that describe the relationship between the system's input and output parameters. Let us consider the main steps of converting to transfer functions. By applying the Laplace transform to the system dynamics equation, the following was obtained:

$$mps^2\theta(s) + bps\theta(s) + mg = \frac{2M(s)}{d_2}\eta_{screw} - f\frac{mg}{cos\alpha} \tag{16}$$

This equation shows how the motor torque affects the angular displacement of the rotor, taking into account mass, damping, and external forces. Solving Equation (15) with respect to $\theta(s)$, the following was obtained:

$$\theta(s)(mps^2 + bps) = \frac{2M(s)}{d_2}\eta_{screw} - f\frac{mg}{cos\alpha} \tag{17}$$

Next, the transfer function of the mechanical part of the system was derived:

$$G_{mech}(s) = \frac{\theta(s)}{M(s)} = \frac{\frac{2\eta_b}{d_2}}{mps^2 + bps} \tag{18}$$

This transfer function describes the response of the mechanical system to changes in the motor torque, taking into account the rotor mass and damping forces. By applying the Laplace transform to Equation (13), the following was obtained:

$$LsM(s) + RM(s) + k_e k_m s\theta(s) = k_m U(s) \tag{19}$$

By deriving the transfer function of the motor, the following was obtained:

$$G_{motor}(s) = \frac{M(s)}{U(s)} = \frac{k_m}{(Ls + R)s + k_e k_m} \tag{20}$$

This transfer function describes the conversion of the input voltage $U(s)$ into the torque $M(s)$, taking into account the electrical parameters of the motor. The complete dynamic model of the system includes both the motor and mechanical system transfer functions:

$$G_{sys}(s) = G_{motor}(s) G_{mech}(s) \tag{21}$$

For numerical calculation and the derivation of the transfer function, a program was developed in Python 3.11.0. The block diagram of the program is shown in Figure 2, and the program output is presented in Figure 3.

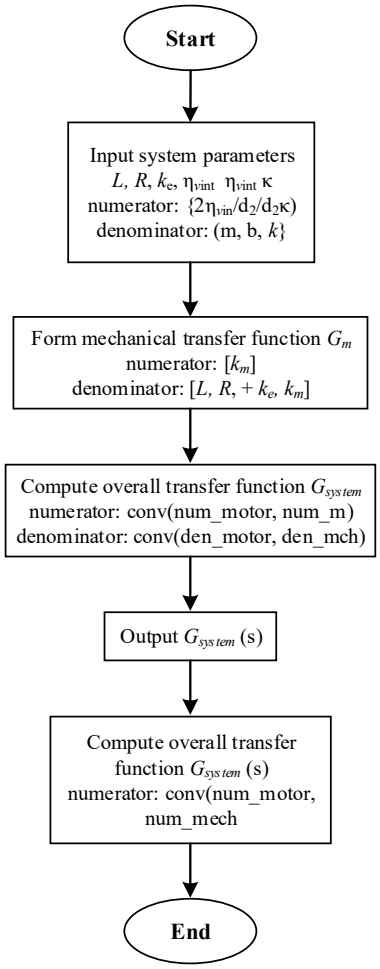


Figure 2. Initial program workflow block diagram.

```
TransferFunctionContinuous(
array([60.71428571])
array([   1.0,  127.0,  255.0, 625.0])
dt: None
)
```

Figure 3. Calculation results.

According to Figure 3, the transfer function of the screw drive control system was obtained:

$$G_{sys}(s) = \frac{60.71}{s^3 + 127s^2 + 255s + 625} \quad (22)$$

The Laplace transform made it possible to represent the system in terms of transfer functions, which significantly simplifies the analysis of its dynamic characteristics and the development of control algorithms. The obtained expressions allow for the investigation of the influence of various system parameters, such as inertia, damping, and the transfer properties of the motor and screw drive. This approach also opens up the possibility for further analysis of system stability and optimization of its performance. The code presented below performs the simulation of the dynamic control system of the screw drive using transfer functions. The objective is to analyze the system's frequency and time responses to assess its stability and efficiency. First, the main system parameters are defined, including the damping coefficient b, motor parameters (inductance, resistance, back EMF and torque constants), and the mechanical parameters of the screw drive. Then, the transfer functions of the mechanical part and the motor are calculated, after which they are combined into the overall system transfer function. The final stage involves analyzing the system's dynamic characteristics. The generated plots help visually interpret the results and determine how effectively the system responds to changes in control input.

The program workflow block diagram is shown in Figure 4.

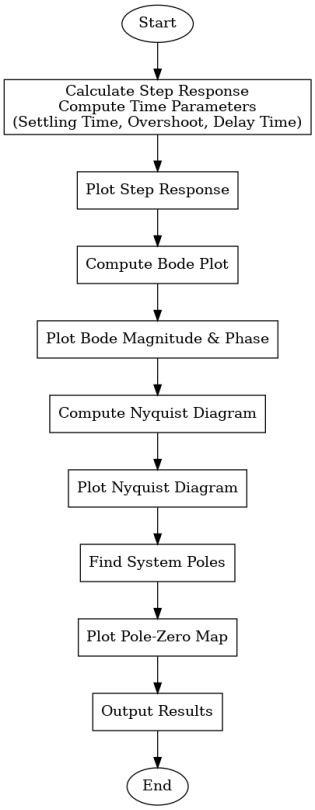


Figure 4. Detailed program workflow block diagram.

The transient response shown in Figure 5 reflects the system's behavior under the influence of a unit step input, allowing for the evaluation of its dynamic performance. This analysis demonstrates how quickly and stably the system responds to a sudden change in the input parameter—a critical factor for drive mechanisms where precise and timely positioning is required.

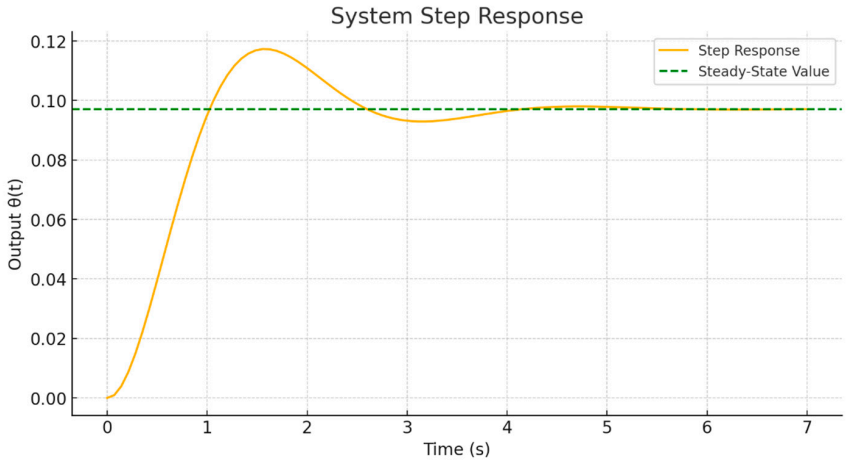


Figure 5. Transient response of the screw drive control system.

The graph shows that after applying a step input, the system exhibits a smooth rise in the output value with a moderate overshoot of approximately 20.8%. The settling time is less than one second (~4 s), indicating a high-speed response. The absence of prolonged oscillations and the rapid achievement of a steady state indicate a sufficient level of damping and proper tuning of the model parameters. This behavior is characteristic of stable systems with a good balance between response speed and the prevention of undesirable oscillations. The frequency response (Bode plot) shown in Figure 6 allows for the assessment of how the system reacts to harmonic signals of varying frequencies. This is important for understanding which frequency ranges pass through the system without distortion and which are attenuated. This is particularly critical for drive systems that are susceptible to external vibrations and noise.

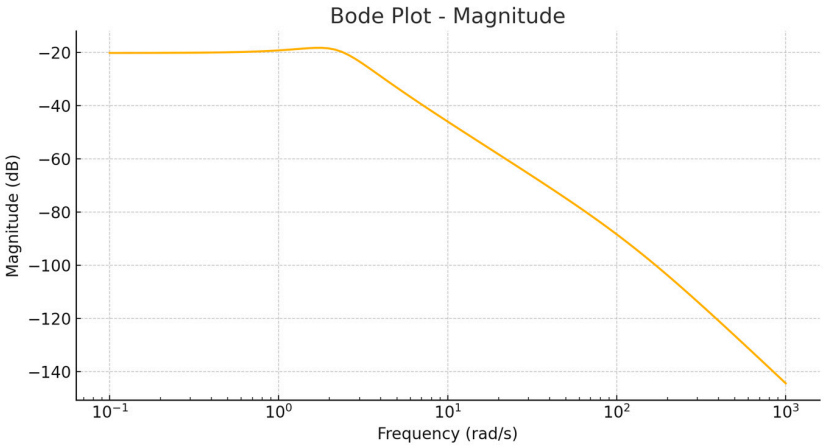


Figure 6. Amplitude–frequency response of the screw drive control system.

The amplitude–frequency response (AFR) graph displays typical low-pass filter behavior: in the low-frequency range, the gain remains stable, allowing the system to effectively respond to slowly varying signals. As the frequency increases, a gradual decrease in amplitude is observed, indicating the system's ability to suppress high-frequency oscillations and noise. The absence of sharp drops and peaks suggests that the system is not prone to resonance phenomena, which enhances its operational reliability. The phase–frequency response (PFR) shown in Figure 7 illustrates the phase shift of the output signal relative to the input as a function of frequency. Analyzing the phase shift allows for the assessment of system behavior under automatic control conditions, where significant phase distortions can lead to reduced stability or even oscillatory modes.

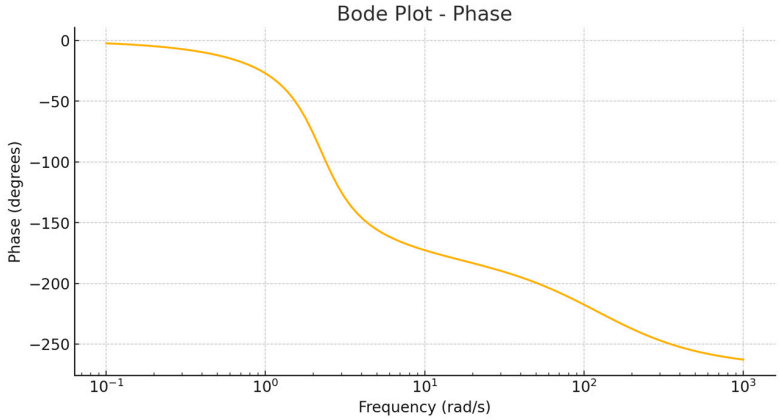


Figure 7. Phase–frequency response of the screw drive control system.

The presented graph shows a smooth decrease in the phase angle as the frequency increases. This behavior is typical for stable systems with a predictable phase shift. The absence of sharp jumps or regions where the phase abruptly crosses critical values (e.g., $-180°$) indicates the system's stability under various frequency influences. Such a phase profile ensures that the system can operate within feedback loops without the risk of losing stability. The Nyquist diagram is a classical tool for analyzing control system stability in the frequency domain. It allows for determining the presence and magnitude of the stability margin through a visual assessment of the curve's position relative to the critical point $(-1, 0)$. In Figure 8, it can be seen that the curve encircles the origin but does not intersect or enclose the critical point. This indicates a stable system with a sufficient stability margin. This behavior confirms that, with the given parameters, the model is not prone to self-excitation and will operate correctly even under changing external conditions or variations in the input signal parameters.

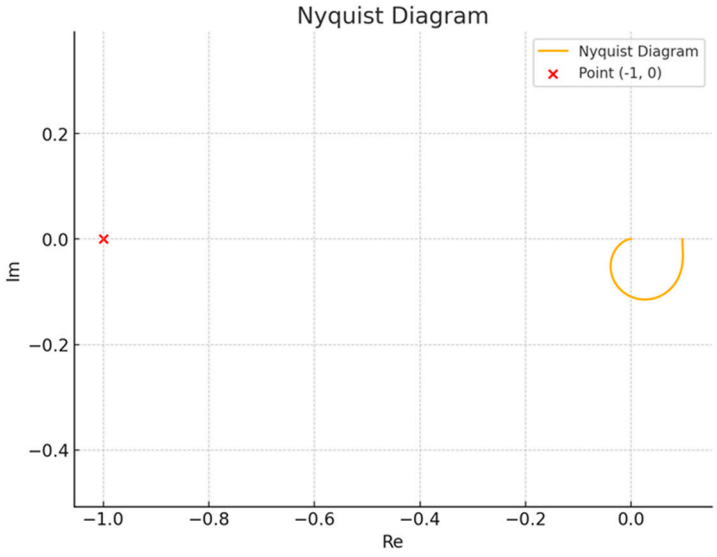


Figure 8. Nyquist diagram of the screw drive control system.

The location of the system poles on the complex plane is a fundamental criterion for assessing stability. Poles located in the left half-plane ensure a decaying system response without sustained oscillations, whereas the presence of poles in the right half-plane would indicate instability. In Figure 9, it is evident that all poles are situated in the left half-plane, fully complying with stability criteria. The presence of complex conjugate poles with negative real parts explains the moderate overshoot observed in the transient response.

This confirms that the system is tuned for an optimal balance between responsiveness and stability.

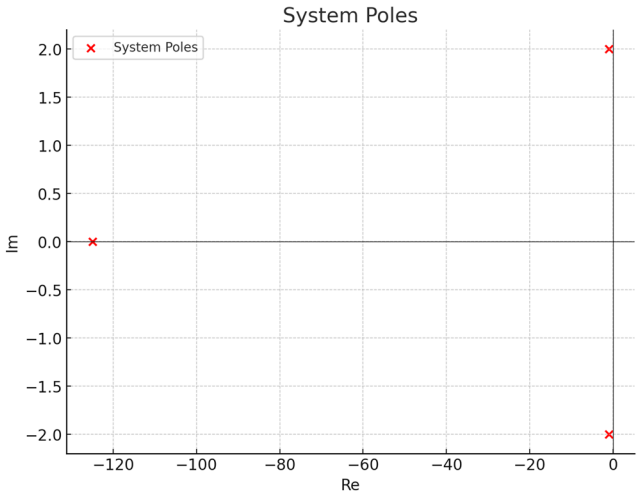


Figure 9. Pole-zero plot of the screw drive control system.

The comprehensive analysis of the dynamic and frequency characteristics of the screw drive control system has confirmed its stability and efficiency. All graphs demonstrate balanced system behavior: rapid response to control inputs, the suppression of high-frequency oscillations, the absence of critical phase distortions, and a significant stability margin. These results indicate the accuracy of the developed mathematical model and its suitability for practical application in automatic rotor height control systems for wind turbines.

4. Conclusions

In the course of this study, a mathematical model of an automatic control system for a screw drive, used to regulate the rotor height of a wind turbine, was developed and analyzed. The use of differential equations followed by Laplace transformation enabled the derivation of transfer functions that accurately describe the dynamics of the electromechanical system. Numerical simulations confirmed the validity of the constructed model: the system demonstrates high stability, fast settling time, and effective suppression of high-frequency oscillations. The analysis of the transient response, amplitude–frequency and phase–frequency characteristics, Nyquist diagram, and pole-zero plot showed that the system possesses a sufficient stability margin and operates reliably under potential external disturbances. The obtained results confirm the effectiveness of the proposed control approach for the screw drive, which enhances rotor positioning accuracy and reduces dynamic loads on the structure. Thus, the presented model and its analysis methodology can be recommended for use in the design and optimization of automatic control systems in wind power installations. Future research should aim to expand the model by incorporating nonlinear effects and environmental parameter variability, as well as conducting experimental validation of the results on a physical test bench or an industrial prototype.

Author Contributions: Conceptualization, A.F. and K.A.; methodology, T.I.; software, A.A.; validation, A.F., K.A. and T.I.; formal analysis, A.A.; investigation, A.F.; resources, T.I.; data curation, K.A.; writing—original draft preparation, T.I.; writing—review and editing, A.F.; visualization, T.I.; supervision, K.A.; project administration, K.A.; funding acquisition, A.A. All authors have read and agreed to the published version of the manuscript.

Funding: This research was funded by the Committee of Science of the Ministry of Science and Higher Education of the Republic of Kazakhstan, grant number BR27195331.

Institutional Review Board Statement: Not applicable.

Informed Consent Statement: Not applicable.

Data Availability Statement: The dataset can be made available upon request from the authors.

Conflicts of Interest: The authors declare no conflicts of interest.

Abbreviations

The following abbreviations are used in this manuscript:

EMF	Electromotive Force
AFR	Amplitude–Frequency Response
PFR	Phase–Frequency Response
VAWT	Vertical-Axis Wind Turbine

References

1. Stoyanov, I.; Iliev, T.; Fazylova, A.; Yestemessova, G. A Dynamic Control Model of the Blades Position for the Vertical-Axis Wind Generator by a Program Method. *Inventions* **2023**, *8*, 120. [CrossRef]
2. Kuo, J.; Pan, K.; Li, N.; Shen, H. Wind Farm Yaw Optimization via Random Search Algorithm. *Energies* **2020**, *13*, 865. [CrossRef]
3. Szeidert, I. Comparative Study Regarding Control of Wind Energy Conversion Systems Based on the Usage of Classical and Adaptive Neuro Fuzzy Controllers. In Proceedings of the 3rd Romanian-Hungarian Joint Symposium on Applied Computational Intelligence (SACI 2006), Timisoara, Romania, 25–26 May 2006; pp. 614–620.
4. Liu, Y.; Zhang, Y.; Sun, K.; Zhao, X. Adaptive Switching Control of Wind Turbine Generators for Necessary Frequency Response. *arXiv* **2020**, arXiv:2005.14562. [CrossRef]
5. Rodrigues, G.; Valério, D.; Melicio, R. Controller Development and Experimental Validation for a Vertical Axis Wind Turbine. *Sustainability* **2022**, *14*, 13498. [CrossRef]
6. Ma, L.; Wang, X.; Zhu, J.; Kang, S. Dynamic Stall of a Vertical-Axis Wind Turbine and Its Control Using Plasma Actuation. *Energies* **2019**, *12*, 3738. [CrossRef]
7. Abdalrahman, G.; Daoud, M.A.; Melek, W.W.; Lien, F.-S.; Yee, E. Design and Implementation of an Intelligent Blade Pitch Control System and Stability Analysis for a Small Darrieus Vertical-Axis Wind Turbine. *Energies* **2022**, *15*, 235. [CrossRef]
8. Fazylova, A.; Alipbayev, K.; Iliev, T.; Aden, A. Advanced Control Strategies for Wind Turbine Blade Pitch Optimization. In Proceedings of the 2024 5th International Conference on Communications, Information, Electronic and Energy Systems (CIEES), Veliko Tarnovo, Bulgaria, 20–22 November 2024; pp. 1–5. [CrossRef]
9. Ali, S.; Park, H.; Lee, D. Structural Optimization of Vertical Axis Wind Turbine (VAWT): A Multi-Variable Study for Enhanced Deflection and Fatigue Performance. *J. Mar. Sci. Eng.* **2025**, *13*, 19. [CrossRef]
10. Chen, L.; Yang, P.; Zhang, B.; Chen, L. Aerodynamic Enhancement of Vertical-Axis Wind Turbines Using Plain and Serrated Gurney Flaps. *Appl. Sci.* **2023**, *13*, 12643. [CrossRef]
11. Sun, G.; Wang, Y.; Xie, Y.; Lv, K.; Sheng, R. Research on the Effect of a Movable Gurney Flap on Energy Extraction of Oscillating Hydrofoil. *Energy* **2021**, *235*, 120206. [CrossRef]
12. Katsaprakakis, D.A.; Papadakis, N.; Ntintakis, I. A Comprehensive Analysis of Wind Turbine Blade Damage. *Energies* **2021**, *14*, 5974. [CrossRef]
13. Costa, Á.M.; Orosa, J.A.; Vergara, D.; Fernández-Arias, P. New Tendencies in Wind Energy Operation and Maintenance. *Appl. Sci.* **2021**, *11*, 1386. [CrossRef]
14. Wang, C.-S.; Chiang, M.-H. A Novel Pitch Control System of a Large Wind Turbine Using Two-Degree-of-Freedom Motion Control with Feedback Linearization Control. *Energies* **2016**, *9*, 791. [CrossRef]

Disclaimer/Publisher's Note: The statements, opinions and data contained in all publications are solely those of the individual author(s) and contributor(s) and not of MDPI and/or the editor(s). MDPI and/or the editor(s) disclaim responsibility for any injury to people or property resulting from any ideas, methods, instructions or products referred to in the content.